International Symposium on Enhanced Solutions for Aircraft and Vehicle Surveillance Applications - ESAVS 2016

Introducing LiDAR Point Cloud-based Object Classification for Safer Apron Operations

Johannes Mund*[1], Frank Michel*[1], Franziska Dieke-Meier[2], Hartmut Fricke[2], Lothar Meyer[2] and Carsten Rother[1]
Technische Universität Dresden
Chair of Air Transport Technology and Logistics
Dresden, Germany
[1]{johannes.mund, frank.michel, carsten.rother}@tu-dresden.de
[2]{dieke-meier, meyer, fricke}@ifl.tu-dresden.de
*Joint First Authors

***Abstract*—Current procedures for conventional and remote airport ground control still rely on the direct (camera-) view. Despite further support by different Radar applications occasional shortcomings in the awareness of the responsible controllers may occur, particularly under adverse weather conditions, giving rise to capacity backlogs, incidents and accidents. As Laser scanners and computer vision algorithms have reached new performance levels in recent years, we proposed a novel concept for complete and independent airport apron surveillance based on LiDAR 3D point data. In this paper we extend our object detection/segmentation technique by addressing object classification in LiDAR 3D scans. We hereby enable LiDAR`s unique capability to classify non-cooperative objects by means of a single sensor and learned model knowledge. Our technique was able to classify and to estimate the poses of an Airbus A319-100 and a Boeing B737-700 parked on the airport apron. In the future we will enhance our classification technique to a wider range of objects including moving ground vehicles and pedestrians.**

Keywords- LiDAR, Laser scanning, 3D point cloud, airport ground surveillance, apron control, aircraft classification, pose estimation

1. INTRODUCTION

Airport ground operations are considered to be significant risk drivers in the aviation sector. Especially the actions that take place on the apron, which is in fact an unstructured working environment with a large variety of objects, substantially contribute to the operational risk. Additionally, various activities of moving aircraft, vehicles, equipment and personnel on a limited space turn the apron into a complex and dynamic system [1] [2] that lends itself to accidents and incidents [3] [4] creating a measurably high risk environment.

Current legacy procedures for apron control rely on the direct view. This principle, however, depends on weather/lighting conditions, resolution limits and the unobstructed line-of-sight. While typical support systems like non-cooperative ground Radar (X and Ku-band) and video cameras are subject to the same or similar conditions, cooperative sensors like Secondary Surveillance Radar (SSR) lack of the capability to detect passive objects like safety-critical foreign object debris (FOD).

Concluding, both the apron`s unique characteristics and (temporary) limitations in the surveillance capabilities inevitably impact the situational awareness of all apron operators. The authors expect the resulting contribution to risk highest in the case of degraded situational awareness[1] at the apron control unit, since it is the overall authority to create and maintain operational safety on the apron.

Motivated by improving the safety level of apron operations beyond current targets (e.g. ICAO A-SMGCS target level of safety [5]), we aim at strengthening the situational awareness of tomorrow's apron control through the first-time provision of three dimensional (3D) data from an independent sensor source.

As laid down in our concept studies in [6] [7], our research approach foresees the development and implementation of a point cloud-based surveillance solution with the capability to recognize present or even emerging hazardous situations by using pattern recognition methods. Assuming that this post-processed 3D point cloud data is provided to the apron controller on an additional screen, he should

[1] Endsley [18] defines situational awareness as "perception of the elements in the environment within a volume of time and space, the comprehension of their meaning and the projection of their status in the near future".

We would like to thank the DFG (German Research Foundation) most sincerely for funding the research presented in this paper (FR 2440/4-1).

be enabled to take corrective actions in time to avoid or manage hazardous situations. Figure 1 depicts the components and key functions of the proposed surveillance concept along with a default apron CWP[2]. Within a currently on-going human-in-the-loop simulation study and a planned in-the-field validation at Dresden airport we will assess the effectiveness of this concept. The central metrics are the number of hazardous situations that could be avoided or safely managed by the apron controller and his reaction times to do so.

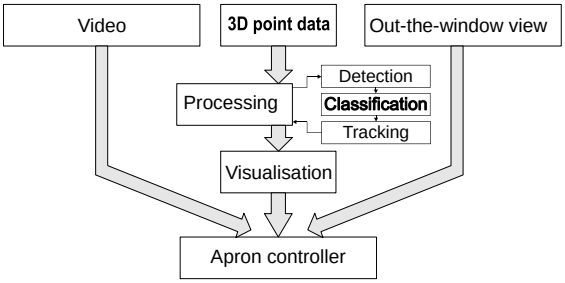

Figure 1. Point cloud-based surveillance concept for apron control with highlighted classification function

In a methodical selection process (refer to [8]) we chose LiDAR-generated sets of real-time processed 3D data points as promising candidate to technically realize our research approach. LiDAR is a non-cooperative Laser beam-based method to calculate distances between the sensor and any reflecting object. It is characterized by its wavelength spectrum from ultraviolet to near-infrared[3] and high frequencies reaching into petahertz range. From LiDAR`s Laser beam properties and additional construction-related factors the following most important advantages over other established airport surveillance sensors[4] result (refer to [8] for details):

- non-cooperative measurement principle
- capability to determine the depth "z" of an object
- good temporal and spatial resolution compared to primary Radar

Based on these features we assume LiDAR to be the most suitable provider of 3D point data as input for the high level pattern recognition technique in our concept. The pattern recognition itself builds on three core functions:

- object detection[5]/segmentation
- object classification[6]
- object tracking

After we had developed a detection/segmentation technique earlier (refer to [8]), this paper goes one step further by proposing a LiDAR point cloud-based classification function and by demonstrating its technical feasibility for two stationary aircraft types.

In section 2, a brief overview about the underlying approach to increase apron safety is provided. This is followed by a short insight into the latest progress made with our detection/segmentation technique serving as fundamental basis for higher level functions, e.g. "classification". Finally, the role and the need for classifying certain objects within our risk mitigation approach is explained.

Section 3 provides insight into the methodological framework for developing a technique to classify aircraft in 3D point data. In the beginning, the most significant challenges for the development of such a technique are summarized. Then, the working principle of the developed classification function is explained, including the generation of training data.

Section 4 demonstrates the technical feasibility of the developed classification function. First, by presenting the results of a small proof of concept study aimed at finding two aircraft models in LiDAR point cloud data recorded at Dresden airport. Second, we report on the conceptual application of the classification function to exemplarily validate an aircraft pushback trajectory model currently under development at TU Dresden. We finally discuss the results in section 5, also taking a look on what needs to be done to reach operational validity in the future.

2. BACKGROUND

In section 1, we introduced the overall motivation to increase the safety level of apron operations. Driven by this motivation, we had been conducting a risk assessment (RA)[7] that delivered us functional requirements for a safety-effective provision of LiDAR point cloud data to the apron controller.

[2] The fusion of 3D point data with sensor input from the existing means of surveillance (Radar, video) will be considered at a later stage of the research.

[3] ≈400nm to ≈3000nm

[4] E.g. video camera, primary surveillance Radar (PSR), secondary surveillance Radar (SSR) and multi-lateration systems (MLAT)

[5] According to Johnson`s theory of discrimination [17] "detection" is about perceiving the "presence of an object"

[6] According to Johnson`s theory of discrimination [17] "classification" is about recognizing the "class to which (an) object belongs […]"

[7] The Functional Hazard Assessment (FHA) of Eurocontrol Safety Assessment Methodology (SAM) [19] served as a methodical framework.

We would like to thank the DFG (German Research Foundation) most sincerely for funding the research presented in this paper (FR 2440/4-1).

2.1. Progress with Object Detection

As a result of the RA, the need for an object detection/segmentation technique as a core function to point cloud-based ground surveillance was confirmed. By means of a hazard and cause analysis that delivered approx. 50 hazards in 3 expert workshops we could lead back 80% of all identified hazards to the presence of at least one physical object/solid target (e.g. aircraft, ground vehicle, FOD.). Therefore, we developed a technique for object detection/segmentation from 3D point cloud data and applied it in a field trial. A detailed report can be found in [8], from where we summarized the following results:

First, the exemplary quantification of the combined detection performance of the tested LiDAR system (*Neptec OPAL 360* LiDAR, TU Dresden detection technique) for 6 test objects and 5 distances proofed the general technical feasibility of our LiDAR system. In particular the results were found promising for rather large objects like aircraft and ground vehicles, whereas the detection of very small objects (e.g. socket wrench) required additional optimization work.

Second, the exemplary analysis on the FOD detection capability proofed our LiDAR system to be able to comprehensively cover and methodically scan a defined apron area for certain FOD types. As an example, a lost suitcase was found in less than 60s in a circular area with ≈84000 m2[8]. This performance stands in contrast to today`s procedures for FOD detection, which rely on random observations from apron personnel and on inspections.

Third, the detection/segmentation technique could not detect moving aircraft and vehicles, and did not feature a real-time visualization. Therefore, our recent effort laid on this last issue, resulting in promising progress: In order to detect and segment object candidates in real-time, we both brought the processes “feature extraction” and “foreground-background segmentation in line with the data acquisition. With computing times less than 0.2s, real-time detection was virtually achieved, while a ring buffer would be continuously providing sensor data[9]. With these improvements, moving aircraft on the apron of Dresden airport could be detected for the first time. Figure 2 shows an experimental graphical user interface (GUI) for the real-time visualization of detected objects. This GUI and the underlying detection/segmentation technique are provided with sensor data from a *Neptec* LiDAR deployed at Dresden airport.

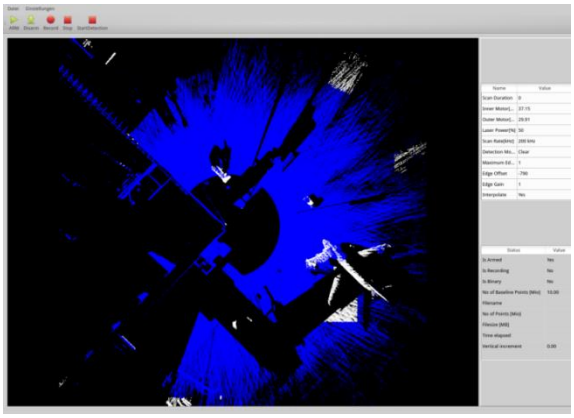

Figure 2. Experimental GUI displaying real-time detection results at Dresden airport, with detected objects coloured in white

2.2. The Role of Object Classification

By analogy to section 2.1, we identified a need for object classification within the proposed LiDAR ground surveillance system.

The development of a function that is able to classify known objects is the next logical step after the foundation had been laid with the latest progress in our detection/segmentation technique. In addition, classification itself is an essential requirement for the next higher level core function: object tracking (refer to Figure 1**)**.

The importance of a function to classify certain objects was also proven from the RA perspective. The hazard analysis conducted could lead back some high severity class (SC)[10] hazards to non- or false classification events. Find below some exemplary hazards (whereas AC stands for aircraft):

- *AC dimensions wrongly perceived* (SC2)
- *AC type wrongly perceived* (SC2)
- *AC type not perceived* (SC5)
- *AC characteristics wrongly perceived* (SC2)
- *Ground equipments' dimensions wrongly perceived* (SC1)
- *Ground vehicle type wrongly perceived* (SC2)
- *Ground vehicle type not perceived* (SC5)

To determine functional requirements with regard to classification, we have to look at this term in detail:

[8] ≈20x the size of a 90m x 45m soccer field

[9] Currently sensor data from the past 30s.

[10] Referring to Eurocontrol SAM the “Severity Class” describes the degree of severity for a hazard`s potential consequence within a range from 1 to 5, where 5 is highest

We would like to thank the DFG (German Research Foundation) most sincerely for funding the research presented in this paper (FR 2440/4-1).

According to Johnson`s definitions[11] the overall classification task is about recognizing the "*class to which (an) object belongs*". Adapting this from our hazard and cause analyses to our approach, this kind of classification is required for aircraft, ground vehicles and pedestrians. *Johnson* defined another, more detailed level called "identification", saying that an "*object is described to limit of an observer`s knowledge*". Adapted to the terminology of the computer vision domain, we named this level "instance recognition". The functional requirements of our RA call for mandatory instance recognition for aircraft and ground vehicles. Finally, it should be noted that *Johnson* also defined the category "orientation", where an object`s "[…] *orientation is determined*". In our approach this is named "pose estimation", representing an intermediate step towards full aircraft classification. This "pose estimation" will be utilized in our exemplary application in subsection 4.2, whereby pose refers to the pose of a known object to the sensor. A summary of all classification (sub-) functions with the corresponding functional requirements can be found in Table 1.

Table 1. Classification (sub-) functions relevant for the development of a classification technique

Johnson`s Theory Category	Johnson`s Theory Examples	Point Cloud Surveillance Adapted Classification Functions	Point Cloud Surveillance Required for
Classifi-cation	Building/ truck/tank/ man	Classification	aircraft/ vehicles/ pedestrians
Identifi-cation	Motel/ pickup truck/T-62 tank/ soldier	Instance Recognition	aircraft: e.g. A319, B737-700 ground vehicles: e.g. Follow me, fuel truck
Orient-ation	e.g. pickup truck abeam to observer	Pose Estimation	→intermediate step to Classification/ Instance Recognition

As we are in a very early development stage of our classification technique we currently limit the requirement definition to these basic functional requirements in Table 1. Once implemented, we particularly will focus on the incorporation of performance requirements, for instance the maximum acceptable delay for our algorithm to provide results for certain object classes ("update rate"). In order to evaluate the results of the proof of concept study for aircraft pose estimation in this paper, we will use the metrics "angular error" and "translational error" (refer to subsection 4.1).

The required classification (sub-) functions in Table 1 (3rd column) clearly underline the unique advantage of LiDAR sensing over other established airport surveillance sensors: Being able to classify objects that do not actively respond to interrogation signals by means of one sensor and fully independent from other sensor inputs.

The above capability is achieved by the combination of two important LiDAR characteristics. First, the non-cooperative measurement principle ensures independence from a target`s active response signal. As such even non-cooperative objects like most general aviation traffic aircraft which are normally not equipped with a Mode-S transponder can be classified.

Second, the high pulse repetition rate (PRR) and high pulse intensities of some LiDAR sensors result in good temporal and spatial resolution compared to common PSR, and even high-resolution millimeter wave Radar. In addition, LiDAR measurements have the capability to determine the depth "z" of an object. The overall result is, that the extraction progress of geometric features from raw data (e.g. spatial dimensions, positions), and thus the extraction of 3D objects from point cloud data, is considerably supported [9] [10]. For instance standard video cameras or infrared are not able to generate information about scene depth, and PSR only measures the slant range.

3. METHODOLOGICAL APPROACH TO OBJECT CLASSIFICATION

3.1. Overview

In the following we explain our approach to classify known objects and to estimate their pose in 3D point cloud data. Compared to the already developed detection/segmentation technique and except for the class "pedestrian", the objects of interest tend to be rather large in our apron scenario: Aircraft, ground vehicles and ground equipment. Figure 3 shows an exemplary LiDAR scan with a clearly visible aircraft silhouette in the background.

[11] Johnson`s theory of visual discrimination [17] is an established model for target acquisition suitable for determining the discrimination quality of electro-opical devices.

We would like to thank the DFG (German Research Foundation) most sincerely for funding the research presented in this paper (FR 2440/4-1).

Figure 3. Exemplary 3D point cloud scan of an airport apron scene

For some of the objects contained in the scan data we have 3D models available. Our aim is to detect those known models and to estimate their pose. Additional objects, which are not of immediate interest, are also present. These objects, along with the ground plane and the airport buildings, constitute the background which should be classified as such.

Before we lay down the working principle of our classification technique in subsection 3.3, we first summarize considerable challenges facing this task.

3.2. Challenges

The classification task poses challenges in the following areas:

A) Apron operations and target objects

Typically, an apron scene is a highly congested environment with many different objects. Furthermore, the heterogeneity within the object classes present at the apron can be large. This contrasts for instance with an automotive scenario from the autonomous driving domain where the heterogeneity within the considered object classes (e.g. cars, pedestrians, bicycles) is rather small. Classification on an instance level is moreover not of interest within the automotive domain. On the apron, however, it is crucial to distinguish between different object instances (refer to Table 1). This "instance recognition" task is particularly difficult when objects appear very similar. For instance, different types of aircraft force the classifier to pick up very subtle details to distinguish between those objects. Since our sensor is immobile we assume the background to be static during the scan. Nevertheless, the background can change between scans and is thus unknown. Furthermore, object occlusion poses a challenge on the task since discriminative object parts may not be visible or the object silhouette may be distorted.

B) LiDAR sensor and point cloud data

We use a *Neptec OPAL 360* LiDAR sensor for capturing the airport apron. The sensor scans the scene by casting out Laser rays in a repetitive pattern. The maximum number of pulses sent per second amounts up to 200000 at a maximum range of 200m. The direction of the rays is determined by two angles, azimuth and elevation. The sensor`s horizontal and vertical FOV are 360° and 45°, respectively [11]. A sensor measurement is defined by the time the pulse needs to travel to the point where it is reflected and send back to the sensor. The sensor gives out sparse 2.5D[12] point clouds as geo-referenced Cartesian coordinates (x,y,z). The percentage return-beam power ratio of every received signal is stored as well[13].

The properties of the sensor data make the task at hand complicated. In analogy to the computer vision community we decided to discretize the sensor readings and map them to a regular 2D pixel grid.

3.3. Techniques

A) Pose Estimation

The task at hand is the classification of known object instances ("instance recognition", see Table 1) $c \in C$ in a 3D point cloud. Additionally the pose H_c of the classified object should be estimated. In the scope of our apron risk mitigation concept objects of interest may be aircraft (e.g. *Airbus 319*, *Boeing 737*), ground vehicles (e.g. Volkswagen T5) and, at a later stage, even pedestrians. For this task of object instance pose estimation the work of Brachmann *et al.* [12] provides state of the art results. Consequently, we adopt their approach to solve the task in an apron scenario.

The aforementioned method can be divided into two parts. In the first step a random forest classifier is used to provide two outputs. However, directly predicting a pose in high dimensional space (6D[14]) is difficult. Therefore, the forest predicts an intermediate representation, the so called object coordinate **y**, for each location in the image (pixel i). An object coordinate represents a local point on the object surface and is therefore three dimensional. The second output of the forest is the object probability $p_i(c)$. The object probability describes the likelihood for an object to be present at a location within the image. From this reason it can be understood as a soft segmentation label. In the

We would like to thank the DFG (German Research Foundation) most sincerely for funding the research presented in this paper (FR 2440/4-1).

[12] The sensor readings can be represented as a surface in 2.5D space and not as a volume in 3D space since the Laser ray is reflected by the first object hit rendering objects behind invisible.

[13] For example, We utilize this value to improve the detection of small objects on the apron within our detection technique introduced in subsection 2.1.

[14] We describe a rigid body transformation in 3D space as [3] rotational and 3 translational parameters (6D).

second step of the method those two outputs are incorporated within a sampling procedure to estimate the pose of the object.

B) Object Coordinate Regression

To realize the first step of the introduced method, we use a random forest to classify pixels of an image. A random forest is a composition of decision trees. Each decision tree is an ensemble of weak classifiers organized in a binary tree structure. To classify a pixel i it is pushed through the tree. At each node features are computed and the outcome determines whether to proceed with the left or the right sub-tree. Finally, the pixel arrives at a leaf node that stores distributions of object probabilities $p_i(c)$ and object coordinates $\mathbf{y}$. Object probabilities from different trees are combined using *Bayes' rule*[15]. Object coordinate predictions are stored by applying mean-shift to all the samples of an object that arrived at the leaf. As a result each tree predicts a distinct object coordinate $\mathbf{y_i}$ $(x, y, z)^T$ for pixel i. Figure 5 (c), (d) depict the object probabilities respectively the object coordinate predictions provided by the tree.

C) Training Data Generation

In order to train the random forest described in *B)*, we need training data showing the objects to be learned in different poses. We generate the training data synthetically since real data is difficult to obtain. We gathered 3D models of the objects from *3D Google Warehouse* (see Figure 4 (a)). An approximation of the sensor model was provided by the sensor manufacturer *Neptec*.

We use a ray tracing based approach to simulate the sensor. Training data is generated by placing the objects on a ground plane and virtually casting rays from the sensor into the scene (see Figure 4 (b)). We only consider viewing positions resting on the objects upper hemisphere. We parametrize the space of viewing positions by three angles: azimuth, elevation and in-plane rotation. To obtain a good coverage we employ slice sampling to distribute the viewpoints equally on the hemisphere. This results in 630 viewing positions.

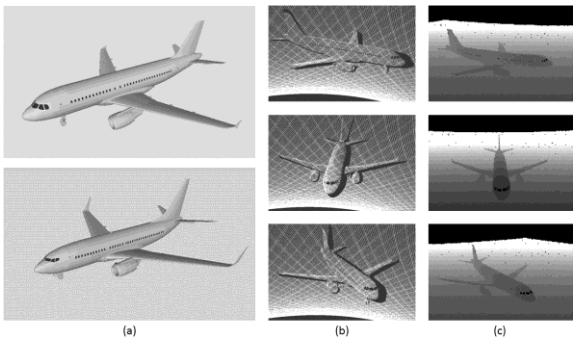

Figure 4. Training data generation. (a): 3D models of two aircraft. Top: Airbus 319-100. Bottom: Boeing 737-700. (b): Point clouds showing different poses of the Airbus 319-100 which were generated through sensor simulation by ray casting. (c): Depth image representation of the point clouds.

D) Pose Hypothesis Generation

To realize the second step of the method mentioned under *A)* we will first introduce the task of 6D pose estimation, formally followed by the description of the hypothesis sampling schema. An illustration of the overall process can be found in Figure 5.

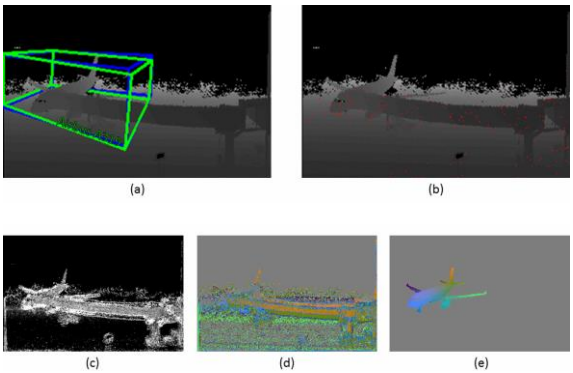

Figure 5. Overview of the classification process. (a): Depth image representation of a 3D scan showing an Airbus 319-100 in parking position. The ground truth[16] 6D pose is depicted by the blue bounding volume. The estimated pose is shown in green. (b): Hypothesis generation process. Sampled hypotheses are projected into the image. Color coding: Hypotheses in red color were rejected by a geometric check. Hypotheses in green were refined. (c): Probability map for the query object. (d): Object coordinate prediction for the query object. (e): Ground truth object coordinates.

The 6D object pose can be described as a rigid body transformation H_c that maps a 3D point in object coordinate space $\mathbf{y} \in Y \subseteq R^3$ onto a point in world coordinate space $\mathbf{x} \in X \subseteq R^3$. The transformation H_c

[15] Mathematical theorem from the theory of probability describing the calculation of conditional probabilities

[16] Ground truth: Information that is ascertained through direct observation.

We would like to thank the DFG (German Research Foundation) most sincerely for funding the research presented in this paper (FR 2440/4-1).

is represented by a homogeneous 4 x 4 matrix consisting of a rotation around the object center followed by a translation. To start the hypothesis sampling we pick a first pixel i_1 within the image based on a weight proportional to the object probabilities $p_i(c)$. We obtain an object coordinate prediction $\mathbf{y}(i_1)$ for the pixel by randomly selecting a tree. Together with the world coordinate $\mathbf{x}(i_1)$ at the pixel i_1 we obtain the first 3D-3D correspondence $(\mathbf{x}(\mathbf{i_1}),\mathbf{y}(\mathbf{i_1}))$ between the object coordinate space and the world coordinate space. Sampling two more pixels within the vicinity of the first pixel i_1 completes the minimal correspondence set. This enables the estimation of H_c using the algorithm by *Kabsch* [13]. Since the depth data as well as the forest predictions are noisy we sample multiple hypotheses and select the best based on a rating function similar to [12].

To evaluate the hypothesis we create a synthetic scan of the object under the estimated pose. The score is calculated by a pixel-wise comparison of the depth values from the sensor, the forest predictions and the synthetically created images. We refine the best 5 hypotheses by recalculating the pose using the inlier set estimated by the rating function. The hypothesis with the best score is chosen as the final pose.

4. DEMONSTRATION

In this section we demonstrate the technical feasibility of our classification technique for which the methodological framework was presented in section 3.

4.1. Proof of Concept

For a small proof of concept study we chose two aircraft types that were to be found by our classification technique in point cloud scans recorded at Dresden airport ("instance recognition" task): An *Airbus A319-100* and a *Boeing B737-700*.

Figure 6. Screenshot from video recording: Airbus A319 (left), B737-700 (right)

We selected both models because of their widespread presence worldwide[17] ensuring a high degree of practical relevance for our test and because of their similar geometrical shape and dimensions to provide a most challenging scenario to the algorithm.

The data recording was done using the *Neptec OPAL 360* LiDAR that had been mounted earlier on the terminal building`s roof at Dresden airport in a total height of approx. 15m (see Figure 7)

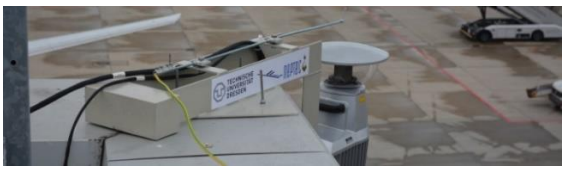

Figure 7. LiDAR sensor mounted at Dresden airport

Both aircraft were recorded in parking position at the same apron stand. After having trained the classification algorithm with both aircraft models, each scan is processed. As a result Figure 8 shows the depth image representation of each aircraft model, demonstrating that the classification for both of them was successful. The ground truth pose annotation of each object was done manually.

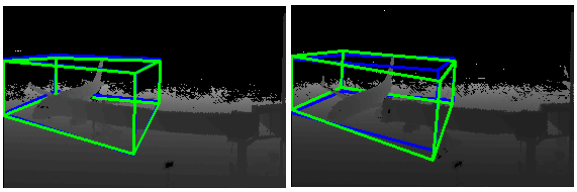

Figure 8. Depth image representation of Airbus A319 (left) and B737-700 (right) in 3D scans

In Table 2 the quality of the classification results is assessed by using the metrics "angular error" and "translational error", respectively. Both metrics can be understood as the achieved "position accuracy": They describe the spatial difference between the pose estimated by the classification algorithm and the ground truth pose, either by the rotational difference (in degree) or the translational difference[18] (in meter) between the green and blue bounding boxes (Figure 8).

Table 2. Achieved classification quality (position accuracy)

Aircraft type	Angular Error	Translational Error
A319-100	1.159°	0.868m
B737-700	3.701°	0.534m

Even though we could not find reference values for "pose estimation" tasks in the field of autonmous

[17] A319 (A320 family total) delivered: 1454 (6932); B737-700 (737 family total) delivered: 1140 (8929)

[18] Translational error (in detail): displacement of the geometrical centre of each bounding box to each other; geometrical centre calculated by Euclidean distance

We would like to thank the DFG (German Research Foundation) most sincerely for funding the research presented in this paper (FR 2440/4-1).

driving, we judge these results as accurate from the *computer vision* perspective. This is also reflected by the plausible bounding volume positions depicted in Figure 8.

From the *Air Traffic Management* (ATM) perspective the following can be stated with regard to our stationary aircraft case: The translational error component of the achieved position accuracy is far lower than the position accuracy required by the ICAO A-SMGCS concept (7.5m for stationary/moving aircraft on the movement area [14]).

Despite these positive results for aircraft classification, validity of this proof of concept study is only given under consideration of the following limitations, leaving much room for further optimizations:

- The 3D model of each aircraft subject to classification must be contained in a data base and needs to be learned in different poses by the algorithm.
- Current computing times of the algorithm are at approx. 3 minutes, which differs greatly from being compliant to functional/performance requirements from the RA.
- Classification of moving aircraft is currently not possible due to the sparse sensor data acquired from dynamic objects.

4.2. Application: Validation concept of a Pushback Trajectory Model

The LiDAR technology and the developed technique to classify objects, in particular aircraft, seem to be appropriate for the validation of a pushback trajectory model that is currently under development at TU Dresden.

At an airport the pushback of an aircraft is necessary when an aircraft has not the ability or is not authorized to leave its stand by its own engine power. In that case, a tow truck (also tug) pushes the aircraft to a defined safe target position at the airport apron (normally on the centerline of the taxiway). These pushback operations hold several risks with regard to injuring ground personnel and damaging aircraft. Therefore, a decision support system is needed to prevent collisions with obstacles and limit/eliminate the number of vulnerable ground assistants [15].

To represent the pushback manoeuver as a safe target setting in the context of system support, a kinematic pushback trajectory model was developed at TU Dresden. This model is able to determine the lateral and longitudinal positions of the nose and main gear reference point of an aircraft as a function of the nose gear deflection angle [16]. Figure 9 exemplarily shows a calculated pushback trajectory of an *Airbus A319* consisting of the trajectories of nose and main gear reference point. For a towbarless[19] pushback the heading of the tow truck represents the deflection of the nose gear.

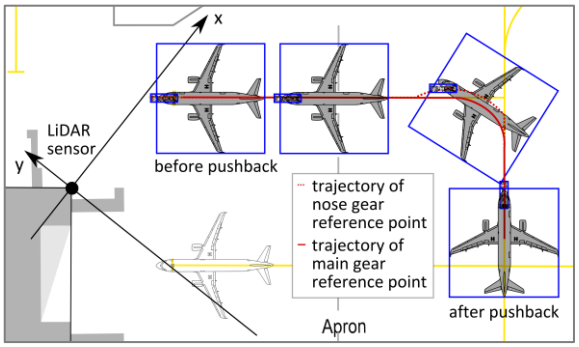

Figure 9. Pushback trajectory for an Airbus A319, consisting of both trajectories described by the nose and the main gear reference point during the pushback manoeuver

To validate the developed pushback trajectory model, a data set is required to determine the position of the aircraft nose gear and main gear reference point for each time step from the beginning to the end of the pushback. Instead of positioning data regarding nose and main gear reference points, (at least) two other reference points and the direction of the aircraft are also adequate to calculate the validation parameters via geometric relations. Further, the respective nose gear deflection angle is needed for validation purposes.

Utilizing the pose estimation functionality of our classification technique, currently the following process states of an exemplary towbarless pushback of an *Airbus A319-100* can be reproduced (also refer to Figure 9):

- *before pushback:* the tow truck is connected to the aircraft`s nose wheel (see Figure 10). The algorithm is able to classify and estimate the pose of the aircraft. The tow truck was manually annotated as the classification algorithm has not been enhanced yet by the object class/instance "tow truck". Nevertheless, the developed algorithm allows this task in principle.
- *after pushback:* aircraft has been pushed to the safe target position and the tow truck is still connected to the aircraft (see Figure 11).

[19] towbarless pushback: the nose gear is directly locked onto a gimbal-mounted platform of the tow truck and lifted then. No towbar (logistic) is needed. In the case of a pushback with towbar, a second center of rotation is given. Hence, the heading of the tow truck does not anymore represent the deflection of the nose gear.

We would like to thank the DFG (German Research Foundation) most sincerely for funding the research presented in this paper (FR 2440/4-1).

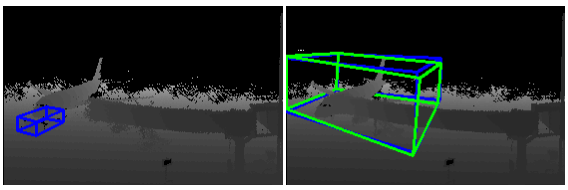

Figure 10. Before pushback: Manually annotated pose of tow truck (blue bounding box) in front of the nose of the Airbus A319 (left), estimated pose of Airbus A319 represented by green bounding box (right)

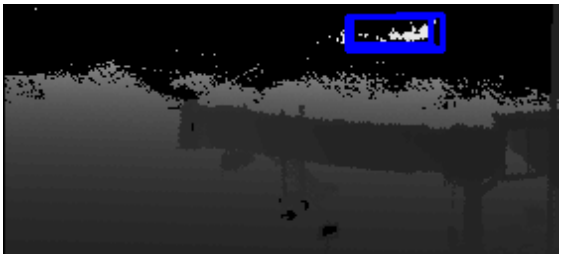

Figure 11. After pushback: Manually annotated[20] pose of Airbus A319-100, whereas the tow truck is not visible in the scan at all (comparing to Figure 10 picture is heightened)

The application of the developed classification technique finally results in coordinates (x; y; z) for each bounding box corner B_k. An exemplary coordinate set for an aircraft *before pushback* can be found in Table 3. Figure 12 illustrates the associated basic geometric relations with regard to the sensor reference point serving as origin of the coordinate system.

Table 3. Estimated coordinates for the bounding box corners of the object aircraft *before pushback*

B_k	x [meter]	y [meter]	z [meter]
B_1	74.1325	-16.8424	-15.5993
B_2	74.0862	-17.0703	-3.42945
B_3	51.0343	-40.4396	-16.1291
B_4	49.9899	6.78191	-15.2491
B_5	50.9879	-40.6675	-3.95928
B_6	26.8916	-16.8153	-15.7789
B_7	49.9435	6.55407	-3.07918
B_8	26.8452	-17.0431	-3.60901

The corner' number (B_k) is set according to a binary approach with '0' as minimum and '1' as maximum of the associated object coordinate (see Figure 12, lower picture).

[20] The distance between the sensor and the aircraft was too high to apply the pose estimation function.

We would like to thank the DFG (German Research Foundation) most sincerely for funding the research presented in this paper (FR 2440/4-1).

These estimated data enable the localization of the pushed aircraft with regard to the sensor reference point. Furthermore, the calculation of the required position of the nose and main gear reference points as well as the deflection angle of the nose gear as function of the tow truck direction can be realized. The remarkable differences of the z-coordinates (Δ 0.35 m) between the surface layered bounding box corners (B_1, B_3, B_4 and B_6) are to be noted. Generally, apron surfaces have a surface slope (maximum 1 per cent), which may responsible for the divergence in the coordinates. Possibly, an imprecise sensor alignment could be another reason.

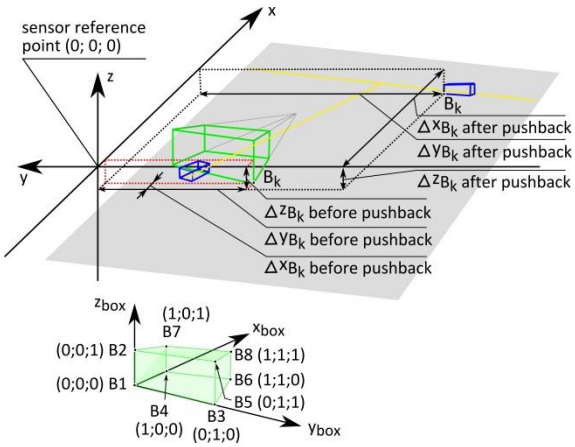

Figure 12. Definition of reference axes and coordinates of the bounding box corners B_k

Currently a complete validation of the developed pushback trajectory model is unfortunately not realizable as the presented algorithm capabilities do not facilitate intermediate states of the pushback at defined time steps. Hence, the next step is to upgrade the current algorithm capabilities in this context. A further problem is the insufficient data quality of the sensor for long distances between sensor and aircraft/tow truck. Therefore, a validation of the pushback trajectory cannot be completely attained. However, for intermediate states of the pushback manoeuver close to the sensor appropriate data should be achievable. Hence, a partly validation of the pushback trajectory model seems to be feasible with an enhanced algorithm and the illustrated validation concept.

5. CONCLUSION & OUTLOOK

This paper introduced a technique to classify objects in LiDAR 3D point data capturing airport scenes. In contrast to our earlier detection/segmentation technique that relied on unlabeled data, we chose a learning-based approach for the classification of known objects. From this it follows that each object to be classified resides in a 3D model data base and has to be learned in different poses by the algorithm.

However, currently we do not have 3D models of each required object at our disposal. One alternative would be the manual generation of these missing object data by directly scanning them at the airport using the LiDAR sensor. This, however, is cumbersome and extremely time-consuming.

Apart from these practical issues, we could demonstrate the good progress of our classification technique by successfully finding an Airbus *A319-100* and a Boeing *B737-700* in the scan data from Dresden airport. For stationary aircraft classification the translational error component of the overall achieved position accuracy (e.g. 0.9m for the *A319*) is far lower than the accuracy demanded by the ICAO A-SMGCS concept (7.5m for stationary/moving aircraft on the movement area [14]). In the demonstration chapter we also used the “pose estimation” feature from our classification technique to present a concept on how to validate a pushback trajectory model where no other practical means has existed before.

However, several issues need to be addressed in order to establish the operational validity of the proposed classification technique. Validity can only be attained if all basic functional requirements previously defined in this paper are met, plus all performance requirements we intentionally did not yet consider in this early development phase. For instance we will have to look at the potential need for “real-time” classification of certain objects, which in terms of the ICAO A-SMGCS concept [14] may result in an “update rate” of 1s and less. With computing times currently in the range of 3 minutes our algorithm is still far away from this state. Nevertheless, we expect the future allocation of the ray tracing method from the central processing unit (CPU) to the graphical processing unit (GPU) as one promising measure.

Closely related to this aspect, we also plan to extend our classification technique to moving objects, for example to aircraft with taxing speeds up to 10m/s in radial/tangential direction. This is another major challenge as the scan principle of the LiDAR sensor we have available only delivers sparse data from those moving objects.

Once all of the above requirements are met by our classification technique, we will finally develop strategies for coping with non-classification events and for avoiding and identifying safety-critical classification errors.

We would like to thank the DFG (German Research Foundation) most sincerely for funding the research presented in this paper (FR 2440/4-1).

Acknowledgment

Our thanks go to Dresden airport for their extraordinary willingness to support our research throughout the whole project duration. We also thank Neptec Technologies for their support.

References

[1] T. Horberry, M. A. Regan and S. R. Toukhsati, "Airport ramp safety and intelligent transport systems," *IET Itelligent Transport Systems*, pp. 234-240, 12 2007.

[2] C. Niessen and K. Eyferth, "A model of the air traffic controller`s picture," *Safety Science* , pp. 187-202, 2001.

[3] Australian Transport Safety Bureau, "Ground operations occurances at Australian airports 1998 to 2008," Canberra, 2010.

[4] Health and Safety Executive, "Aircraft turnround," Sudbury, 2000.

[5] ICAO, "Safety Management Manual doc 9859".

[6] L. Meyer, J. Mund, B. Marek and H. Fricke, "Performance test of LiDAR point cloud data for the support of apron control services," in *Proceedings of the International Symposium on Enhanced Solutions for Aircraft and Vehicle Surveillance Applications (ESAVS)*, Berlin, Germany, 2013.

[7] J. Mund, L. Meyer and H. Fricke, "LiDAR Performance Requirements and Optimized Sensor Positioning for Point Cloud-based," in *Proceedings of the 6th International Conference on Research in Air Transportation*, Istanbul, Turkey, 2014.

[8] J. Mund, A. Zouhar, L. Meyer, H. Fricke and C. Rother, "Performance Evaluation of LiDAR Point Clouds towards Automated FOD Detection on Airport Apron," in *International Conference on Application and Theory of Automation in Command and Control Systems (ATACCS)*, Toulouse, 2015.

[9] A. Friedrich, “Evaluierung von Methoden zum Erstellen und Aktualisieren von sicherheitskritischen Flughafendatenbanken nach RTCA Do-272a, TU Darmstadt, 2008.

[10] B. Zhang, W. Smith and S. Walker, "3-D Object recognition from point clouds," in *Proceesdings from ILMF*, 2011.

[11] Neptec Technologies , "OPAL-360 Sensor 2.0. User Manual," 2013.

[12] E. Brachmann, A. Krull, F. Michel, S. Gumhold, J. Shotton and C. Rother, "Learning 6d object pose estimation using 3d object coordinates," in *European Conference on Computer Vision (ECCV)*, Zurich, 2014.

[13] W. Kabsch, "A solution for the best rotation to relate two sets of vectors," in *Acta Crystallographica Section A*, 1976.

[14] International Civil Aviation Organization (ICAO), "Advanced Surface Movement Guidance and Control Systems (A-SMGCS) Manual. Doc 9830," ICAO, Montral, 2004.

[15] F. Dieke-Meier and H. Fricke, "The need for a collision prevention system for the push back of aircraft," in *Proceedings of International Council of the Aeronautical Sciences*, Brisbane, Australien, 2012.

[16] F. Dieke-Meier and H. Fricke, "Modeling aircraft pushback trajectories for safe operations," in *International Conference on Application and Theory of Automation in Command and Control Systems (ATACCS)*, Naples, 2013.

[17] J. Johnson, Analysis of Image Forming Systems, 1958.

[18] M. Endsley, "Design and Evaluation for Situation Awareness," 1988.

[19] ESARR SRC, "Eurocontrol safety regulatory requirement 4 - risk assess-ment and mitigation in ATM," Eurocontrol, Brussels, BE, 2001.